Revised Version

Phys. Rev. D 76; 074021 (2007)
BUHEP-07-01
CPT-P05-2007
DESY 07-008
WUB/07-01

BUHEP-07-01, CPT-P05-2007, DESY 07-008, WUB/07-01

Diquark correlations in baryons on the lattice with overlap quarks

Ronald Babich,[1] Nicolas Garron,[2] Christian Hoelbling,[3] Joseph Howard,[1] Laurent Lellouch,[4] and Claudio Rebbi[1,*]

[1] *Department of Physics, Boston University, 590 Commonwealth Avenue, Boston MA 02215, USA*
[2] *DESY, Platanenallee 6, D-15738 Zeuthen, Germany*
[3] *Department of Physics, Universität Wuppertal, Gaussstr. 20, D-42119 Wuppertal, Germany*
[4] *Centre de Physique Théorique, CNRS Luminy, Case 907, F-13288 Marseille Cedex 9, France*[†]

(Dated: January 25, 2007)

We evaluate baryon wave functions in both the Coulomb and Landau gauge in lattice QCD. These are constructed from quark propagators calculated with the overlap Dirac operator on quenched gauge configurations at $\beta = 6$. By comparing baryon states that differ in their diquark content, we find evidence for enhanced correlation in the scalar diquark channel, as favored by quark models. We also summarize earlier results for diquark masses in the Landau gauge, casting them in a form more easily compared with subsequent studies.

PACS numbers: 11.15.Ha 12.38.-t 12.38.Gc 14.20.-c

arXiv:hep-lat/0701023v2 19 Oct 2007

I. INTRODUCTION

The notion of a diquark is nearly as old as that of quarks themselves and has been invoked to explain many aspects of hadron phenomenology (see [1] for a review). Most generally, a diquark is any two quark system, but the term is more often taken to denote two correlated quarks in a particular representation of flavor and spin. In QCD-inspired quark models [2], the color-hyperfine interaction gives rise to attraction in the spin singlet, SU(3)-flavor anti-triplet channel, a configuration known as a scalar diquark or more evocatively as a "good" diquark. In contrast, the spin triplet, flavor sextet channel is repulsive, and the associated axial vector or "bad" diquark is disfavored. Note that in this discussion and the rest of the paper, we only consider positive-parity diquarks in the $\bar{3}$ of color, as would describe two valence quarks in a baryon. While one may write down diquark operators symmetric in color, all evidence points toward their being energetically disfavored.

In recent years, diquarks have received increased attention in light of the possible existence of exotic states such as the Θ^+, as diquark models make definite predictions for their properties [3]. The status of the Θ^+ remains uncertain (see [4] for a recent review of the experimental situation), but it serves to remind one of the relative lack of other exotics naively allowed by QCD, a scarcity that may largely be explained if diquark correlations play an important role in hadron structure [5].

Ideally, issues such as these should be addressed by direct appeal to the fundamental theory. The lattice is the principal calculational framework for nonperturbative QCD and has been brought to bear on the question of diquarks in several recent studies (we set aside direct searches for exotic states). Perhaps the most straightforward approach is to construct a diquark two-point function and consider its fall-off in time, as one does to extract hadron masses. A diquark by itself is not a color singlet, however, and so one must either fix the gauge or introduce an additional source of color. The former approach was first pursued in [6], where diquark correlators were calculated with Wilson fermions in the Landau gauge. More recently, we presented a similar investigation in [7] with overlap fermions at significantly lighter quark masses. By comparing the effective mass of the diquark with that of its constituent quarks, the scalar diquark was found to be bound in the limit of vanishing quark mass. In Section IV below, we briefly summarize these results in order to give values for mass splittings that may be more easily compared with subsequent studies. In the second approach, one constructs a gauge invariant object by contracting the free color index of the diquark at source and sink with a Wilson line, serving as a static quark [8, 9]. This allows one to extract diquark mass differences, in qualitative agreement with the fixed-gauge approach. See also [10], where point-to-point baryon correlators containing various diquarks are compared to those in the free theory.

While useful, such mass determinations provide limited information about the nature of diquark correlations. In this work, we directly investigate spatial correlations among quarks in baryons by calculating baryon wave functions on the lattice. At least two natural formalisms exist for defining what is meant by a "wave function." The one pursued here begins with a standard baryon correlator and involves displacing quarks at the sink. This function of quark displacements is then evaluated in a fixed gauge [11]. A very early study of such wave functions may be found in [12] and more complete investigations in [13, 14]. These treat only a subset of all possible quark displacements and are largely motivated by a desire for improved interpolating operators for spectroscopy. Nevertheless, and although not emphasized, the nucleon wave function parametrized in [13, 14] does exhibit characteristics attributable to diquark effects, in particular a negative charge radius for the neutron.

*rebbi@bu.edu
[†] CPT is "UMR 6207 du CNRS et des universités d'Aix-Marseille I, d'Aix-Marseille II et du Sud Toulon-Var, affiliée à la FRUMAM."

An alternative definition of a hadronic wave function is that provided by the density-density correlator method [15, 16, 17]. A recent addition to the body of work treating such correlation functions for baryons [18, 19, 20] may be found in [21], where the focus is on possible deformations arising from spin-orbit coupling. Finally, a very recent study [9] employs the density-density correlator technique to examine the wave function of a diquark constrained to a spherical shell about a static quark, a gauge-invariant setup mentioned above in the context of diquark mass differences. By fitting to an exponential ansatz, the authors of [9] find a large, but finite, radius for the scalar diquark in this environment.

In this work, we present the first detailed study of diquark correlations in physical baryons (with all quark masses finite). We consider all possible displacements of the three quarks and calculate wave functions in both the Coulomb and Landau gauges. By directly comparing wave functions of disparate states and calculating ratios of mean quark separations, we find evidence of enhanced correlation in the scalar diquark channel. We work in quenched QCD and employ the overlap Dirac operator [22, 23, 24, 25] in our calculation, a discretization which preserves chiral symmetry on the lattice [26, 27] and is thereby closest to the continuum formulation.

The paper is organized as follows. In Section II, we provide details of our calculation and describe the correlation functions and states that we study. In Section III and its subsections, we present and compare our baryon wave functions and from them calculate values for mean quark separations. Finally, in Section IV, we calculate diquark mass differences from data first presented in [7].

II. DETAILS OF THE CALCULATION

This study is one in a series employing the overlap Dirac operator on a large lattice. Results for meson and baryon spectra, as well as meson wave functions, diquark correlators, and other observables were presented in [7]. In [28], we calculated matrix elements relevant for kaon physics in the standard model and beyond with a careful treatment of nonperturbative renormalization in the RI/MOM scheme. We direct the reader to [7] for a discussion of the many advantages of the overlap discretization as well as for details of our implementation beyond those given here.

The overlap Dirac operator describing a massless quark [23] is given by

$$D = \frac{\rho}{a}\left(1 + \frac{X}{\sqrt{X^\dagger X}}\right), \qquad (1)$$

where $X = D_W - \rho/a$ is the Wilson Dirac operator with mass $-\rho/a$. It follows that inversion of the overlap operator requires the repeated calculation of $1/\sqrt{X^\dagger X}$. This is accomplished with polynomial or rational function approximations and is very demanding computationally. An unquenched calculation on a lattice as large as ours would be beyond the capability of presently available resources. We therefore work in the quenched approximation and note that prior experience with Wilson fermions has shown hadronic wave functions of the type we study to be largely unaffected by quenching [14].

We employ the Wilson gauge action with $\beta = 6$ on a lattice of size $18^3 \times 64$. This gives an inverse lattice spacing a^{-1} of 2.12 GeV [29, 30] on the basis of the Sommer scale defined by $r_0^2 F(r_0) = 1.65$ with $r_0 = 0.5$ fm [31]. One hundred independent gauge configurations were generated and then fixed to the Landau gauge before inverting the Dirac operator. The negative mass parameter in the definition of the overlap was set to $\rho = 1.4$ in order to maximize locality [32]. Quark propagators were calculated from a point source for all color-spin combinations with a conjugate gradient multimass solver for bare quark masses $am_q = 0.03, 0.04, 0.06, 0.08, 0.10, 0.25, 0.50, 0.75$. For reference, corresponding values of the pion mass as well as baryon masses are given in Table I [7].

We now describe the states that we study. We work in a Dirac basis where γ_4 is diagonal and utilize "nonrelativistic" wave functions involving only either upper or lower spinor components. Labeling the three quarks u, d, s for convenience, we give the spin structure of the states of interest in Table II in a transparent notation. In the SU(3) classification, these correspond to the octet Λ and Σ states and the decuplet Σ^*. In Section III, we will find it most illuminating to compare the Λ to the Σ^*; in the former, the u and d are in a spin-0 "good diquark" configuration, while in the latter they are in a spin-1. The octet Σ is a cousin of the nucleon in which the pairs u, s and d, s are in superpositions of spin-0 and spin-1.

For a given state, with spin structure as given in the table, we construct a zero-momentum correlator

$$G(\vec{r}_u, \vec{r}_d, t) = \sum_{\vec{r}} \langle u(\vec{r}+\vec{r}_u, t) d(\vec{r}+\vec{r}_d, t) s(\vec{r}, t) \times \bar{u}(\vec{0}, 0) \bar{d}(\vec{0}, 0) \bar{s}(\vec{0}, 0) \rangle . \qquad (2)$$

Here color indices are implicit and are contracted with the antisymmetric tensor at source and sink. We combine correlators for the (two for the octet, four for the decuplet) spin states distinguished by J_z. Finally, to the forward-propagating correlators constructed with upper spinor components we add correlators propagating in

am_q	aM_P	aM_8	aM_{10}
0.03	0.219(3)	0.63(2)	0.75(3)
0.04	0.247(2)	0.66(2)	0.78(2)
0.06	0.297(2)	0.714(11)	0.82(2)
0.08	0.340(2)	0.763(9)	0.868(12)
0.10	0.3803(14)	0.810(7)	0.909(10)

TABLE I: Masses, in lattice units, of the lightest pseudoscalar meson, octet baryon (e.g. nucleon), and decuplet baryon for quarks of equal mass am_q. Quoted errors are statistical only.

Λ	$(u_\uparrow d_\downarrow s_\uparrow - u_\downarrow d_\uparrow s_\uparrow)/\sqrt{2}$
	$(u_\downarrow d_\uparrow s_\downarrow - u_\uparrow d_\downarrow s_\downarrow)/\sqrt{2}$
Σ	$(u_\uparrow d_\downarrow s_\uparrow + u_\downarrow d_\uparrow s_\uparrow - 2u_\uparrow d_\uparrow s_\downarrow)/\sqrt{6}$
	$(u_\downarrow d_\uparrow s_\downarrow + u_\uparrow d_\downarrow s_\downarrow - 2u_\downarrow d_\downarrow s_\uparrow)/\sqrt{6}$
Σ^*	$u_\uparrow d_\uparrow s_\uparrow$
	$(u_\downarrow d_\uparrow s_\uparrow + u_\uparrow d_\downarrow s_\uparrow + u_\uparrow d_\uparrow s_\downarrow)/\sqrt{3}$
	$(u_\uparrow d_\downarrow s_\downarrow + u_\downarrow d_\uparrow s_\downarrow + u_\downarrow d_\downarrow s_\uparrow)/\sqrt{3}$
	$u_\downarrow d_\downarrow s_\downarrow$

TABLE II: Baryon states.

the backward time direction that have been constructed with lower components. We thereby double our statistics while ensuring that only the desired positive-parity states are excited from the vacuum.

Since the quarks at the sink may be taken to be at distinct spatial sites, Eq. (2) is only well-defined if we specify the gauge. In Section III we evaluate this correlation function in both the Coulomb and Landau gauges. Coulomb gauge-fixing was performed using simulated annealing, starting from gauge configurations already fixed to the Landau gauge. At sufficiently large times, $G(\vec{r}_u, \vec{r}_d, t)$ settles into a spatial profile that is independent of t up to normalization. We refer to this profile as the "wave function,"

$$\Psi(\vec{r}_u, \vec{r}_d) = \frac{G(\vec{r}_u, \vec{r}_d, t)}{\sqrt{\sum_{\vec{r}_u, \vec{r}_d} |G(\vec{r}_u, \vec{r}_d, t)|^2}} \,. \qquad (3)$$

This zero-momentum wave function in general depends on two 3-vectors, i.e. six numbers. As discussed in the next section, however, we only resolve a dependence on separations between pairs of quarks, and it is therefore effectively a function of a triangle, parametrized by three numbers. For the purpose of displaying the wave function, we adopt the geometry shown in Fig. 1. Here z is the distance between the quark labeled by s and the center of mass of u and d. The axis determined by z is taken to establish a coordinate system in which we specify the position (x, y) of u with respect to the center of mass. We note that the states we consider are all symmetric under interchange of the positions of u and d. In summary, the wave function in these coordinates is given by

$$\begin{aligned}\Psi(x,y,z) \;=\; & \sum_{\vec{r}_u}\sum_{\vec{r}_d} \frac{\Psi(\vec{r}_u,\vec{r}_d)}{\Psi(\vec{0},\vec{0})}\delta\left(z - \frac{1}{2}|\vec{r}_u + \vec{r}_d|\right) \\ & \times \delta\left(y - \frac{(\vec{r}_u - \vec{r}_d)\cdot(\vec{r}_u + \vec{r}_d)}{2|\vec{r}_u + \vec{r}_d|}\right) \\ & \times \delta\left(x - \sqrt{\frac{1}{4}|\vec{r}_u - \vec{r}_d|^2 - y^2}\right) \,, \qquad (4)\end{aligned}$$

where we have normalized the amplitude to unity where all three quarks are at the same site and have defined the delta function on the lattice taking into account the multiplicity of the sites. In constructing the wave function, we only consider configurations of the quarks where no two are separated by more than half the length of the lattice ($L/2 = 9a$).

We conclude this section with some final details of our implementation. First, we note that it might be advantageous to replace the point source in Eq. (2) with an extended operator that better overlaps the desired state. We were constrained in our calculation, however, by the fact that point-source propagators were required for studies of nonperturbative renormalization and weak matrix elements; the calculation of an additional set of smeared-source propagators was deemed too costly to be worthwhile.

The wave functions we present in Section III were calculated by summing over all possible positions of the three quarks. Since each sum is over 18^3 sites, this involves a nontrivial amount of work. We were able to greatly speed up the calculation, however, by employing a fast Fourier transform and utilizing the convolution theorem to eliminate one of the summations. A related issue is the large amount of data that would have to be stored to capture all possible relative displacements of the quarks (i.e. all possible embeddings of a triangle in the lattice). This was avoided by adopting the parametrization described above and building a histogram in the x, y, z coordinates with linear interpolation. The bin size was taken to be $0.225a$ in x, y and $0.45a$ in z, sufficiently small that the mean quark separations presented in Section III B are unbiased, as confirmed by examining the totally symmetric Σ^* state.

Computations were performed with shared memory code on IBM p690 systems at Boston University and NCSA.

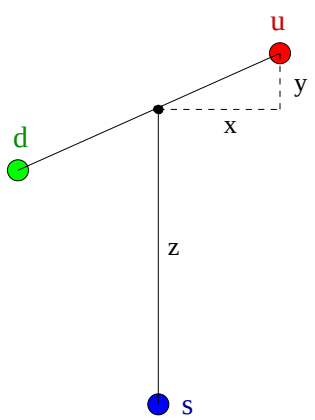

FIG. 1: Geometry for visualizing the wave functions.

III. BARYON WAVE FUNCTIONS

A. Wave functions

Visualization of the wave functions will prove to be quite useful for discerning differences in spatial correla-

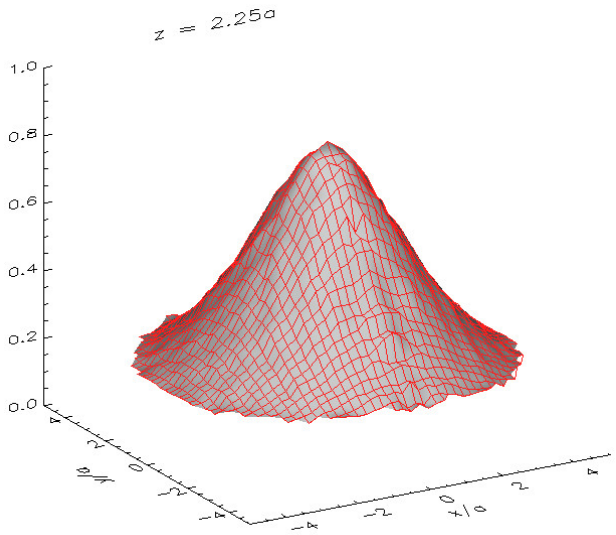

FIG. 2: (Color online) Wave function of the Λ evaluated at $t = 10a$ in the Landau gauge, for $z = 2.25a$.

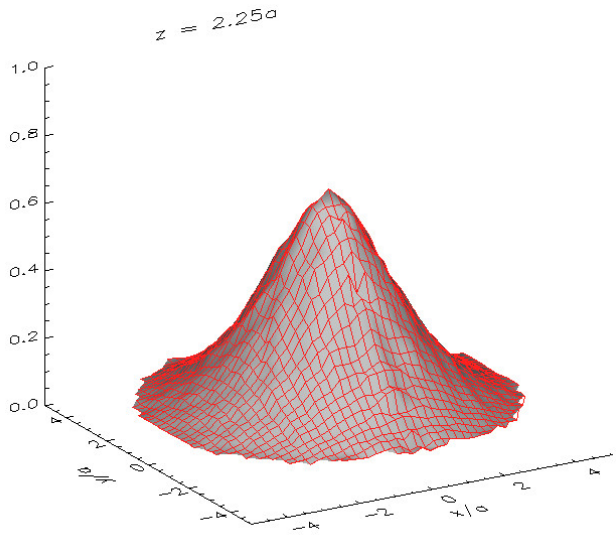

FIG. 3: (Color online) Wave function of the Λ evaluated at $t = 10a$ in the Coulomb gauge, for $z = 2.25a$.

tions between states. As a first step, we must choose the time t at which to evaluate the wave function. For small times, the correlator $G(\vec{r}_u, \vec{r}_d, t)$ in Eq. (2) is dominated by excited states. It is therefore necessary to take t sufficiently large that the spatial profile has settled into that of the ground state. We find that for the states we study, the wave function has settled by $t = 8a$, in agreement with what was observed for effective masses when calculating baryon spectra [7]. We conservatively take $t = 10a$ in the remainder of this paper.

For plotting purposes, we fix z, the distance between the center of mass of the first two quarks and the position of the third. In Fig. 2, we plot the Λ wave function in the Landau gauge as a function of x, y for one such z separation. All three quark masses are taken to be $am_q = 0.03$, the lightest available value. The corresponding wave function in the Coulomb gauge is plotted in Fig. 3. Recall that the wave functions have been normalized to 1 where all three quarks are at the same site ($x = y = z = 0$, not shown). Figures 2 and 3 exhibit the general property that Coulomb-gauge wave functions are less broad and better contained in the lattice volume than those calculated in the Landau gauge, in agreement with [13, 14]. We will focus on Coulomb-gauge wave functions in the remainder of this section.

Statistical errors, which for clarity are not shown in Figs. 2-5, are on the order of 6 to 10 percent (see Fig. 6 below). It is noteworthy that the overall amplitude of the wave function tends to vary configuration by configuration while it maintains the same basic shape. In other words, if the wave function at its peak (always at $\vec{r}_u = \vec{r}_d = 0$) is found to be larger than average on a given gauge configuration, it is likely to be larger at all other quark displacements on that configuration. In [13, 14], this effect was taken as motivation to normalize the wave functions on a per-configuration basis. While effective, this approach is difficult to justify from a field-theoretic perspective and we do not pursue it here. We note, however, that when comparing the properties of various wave functions quantitatively, such contributions to the errors often cancel, as we find for mean quark separations in the next section.

By parametrizing our wave functions in terms of relative separations, without regard to orientation, we have implicitly assumed isotropy. Of course, one recognizes that there is a preferred direction, the z-direction of the lattice (not to be confused with our z coordinate) with respect to which the z-component of spin is defined. To test for the possible presence of spin-orbit coupling, we added a fourth dimension to our histogram with the new variable being the projection of the vector whose length we call "z" along the z-direction of the lattice. We then constructed a wave function with definite J_z and looked for a dependence on this variable. Within errors, we found no evidence for such a dependence. We conclude that the effects of spin-orbit coupling, if present, are below the statistical limits of our calculation.

We come now to the main point of interest. For the Λ state whose wave function is plotted in Fig. 3, the u, d quarks are in the spin-0, "good diquark" configuration. We would like to compare this wave function to that of the Σ^*, where the two quarks are in the spin-1 configuration. In Fig. 4 and Fig. 5, we plot the two wave functions together for two different z separations. A cross-section of Fig. 4 with $y = 0$ is shown in Fig. 6 to give an indication of the errors. As predicted in the literature, we note significantly stronger clustering when u, d are in the good diquark configuration. This feature is independent of z.

In this section, we have presented results for baryons

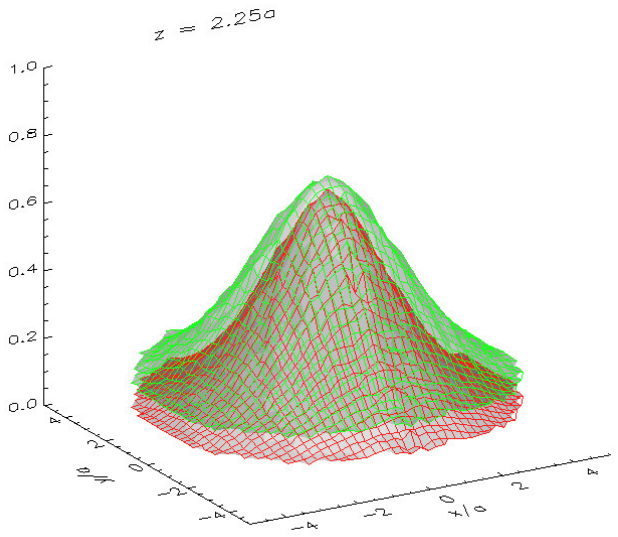

FIG. 4: (Color online) Comparison of Λ (red) and Σ^* (broader, in green) wave functions in the Coulomb gauge, for $z = 2.25a$.

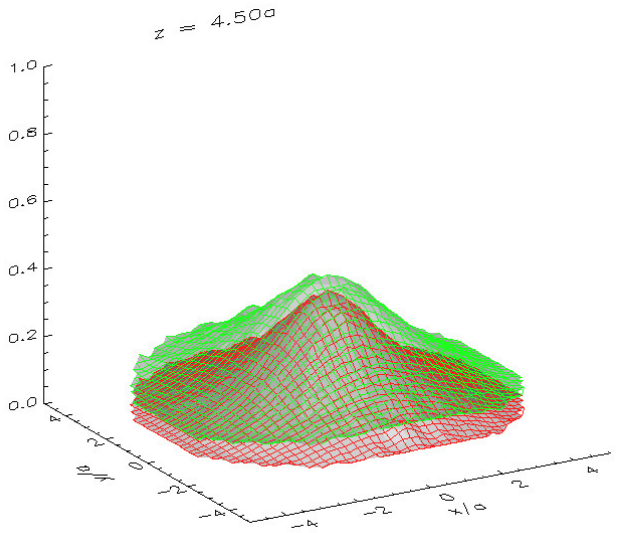

FIG. 5: (Color online) Comparison of Λ (red) and Σ^* (broader, in green) wave functions in the Coulomb gauge, for $z = 4.50a$.

where the three quarks are taken to be degenerate in mass with $am_q = 0.03$. In the next section, we will evaluate the effect of increasing this mass. One may also consider baryons where the s quark is taken to be significantly heavier than the others. None of the qualitative features are changed, but we do observe a slight tendency for the mean separation between the two light quarks to be larger than that between one of the light quarks and the heavy quark, when considering the otherwise symmetric Σ^* state. This is a purely kinematic effect that would apply even in a classical system of one heavy and two light particles bound by two-body interactions.

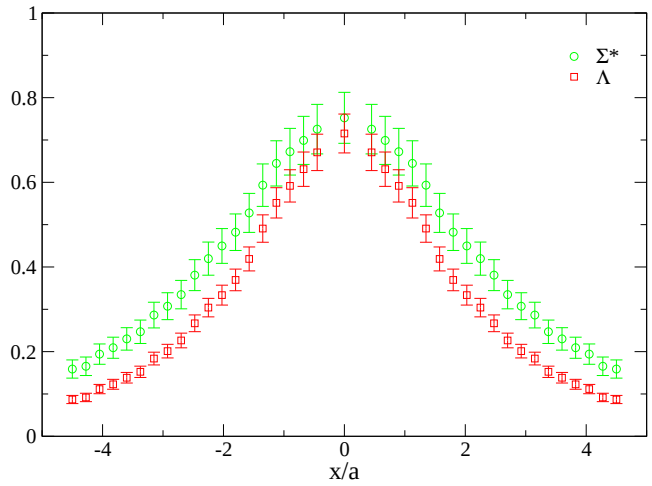

FIG. 6: (Color online) Cross-sections of Λ and Σ^* wave functions with $z = 2.25a$ and $y = 0$.

B. Mean quark separations

From our wave functions, we calculate the mean square separation between the u and d quarks in the natural way:

$$\langle |\vec{r}_u - \vec{r}_d|^2 \rangle = \sum_{\vec{r}_u} \sum_{\vec{r}_d} |\Psi(\vec{r}_u, \vec{r}_d)|^2 \, |\vec{r}_u - \vec{r}_d|^2 \,. \qquad (5)$$

Similarly, noting that our coordinates are defined such that $\vec{r}_s = 0$,

$$\langle |\vec{r}_u - \vec{r}_s|^2 \rangle = \sum_{\vec{r}_u} \sum_{\vec{r}_d} |\Psi(\vec{r}_u, \vec{r}_d)|^2 \, |\vec{r}_u|^2 \,. \qquad (6)$$

Since our baryons reside in a finite volume, such mean separations must be interpreted with care. In particular, we do not take into account the tails of the wave functions that extend into adjacent cells of our periodic lattice, nor do we remove those that impinge from them. To do so would require that we model and fit the numerical wave functions. In contrast, the separations that we calculate follow directly from the data. In the large volume limit, these separations would converge to definite values. In our finite volume, they provide a rough quantitative estimate of the clustering observed in the scalar diquark channel and of the dependence of such clustering on quark mass. To the extent that finite volume effects are present, they are expected only to weaken correlations. In Tables III and IV in the appendix, we collect root mean square separations for the various states in the

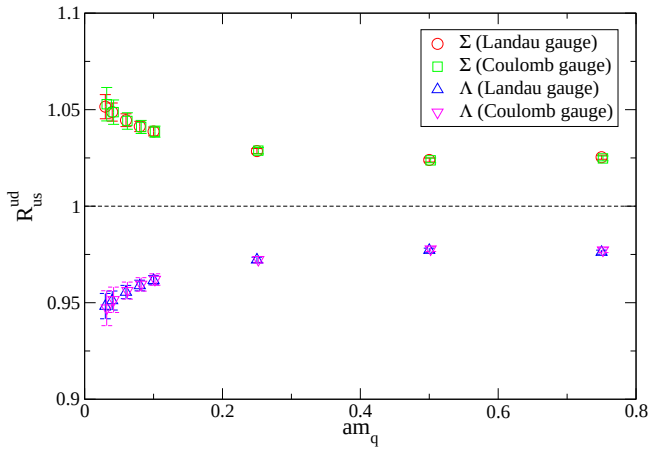

FIG. 7: (Color online) Ratios of RMS quark separations as a function of bare quark mass am_q.

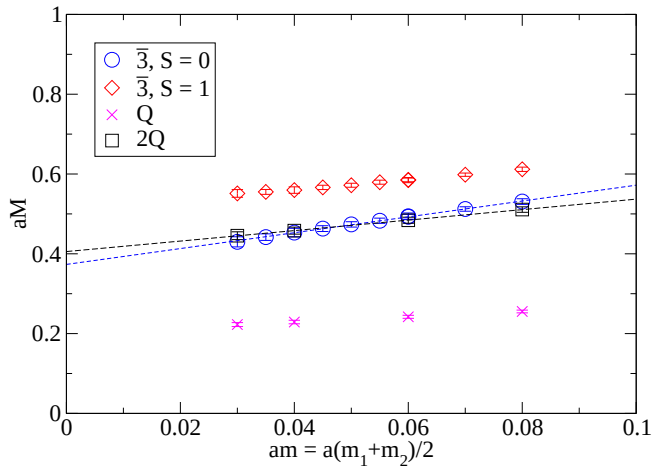

FIG. 8: (Color online) Constituent quark and diquark masses in the Landau gauge, taken from [7].

two gauges. Errors have been calculated via the bootstrap method with 500 samples.

In QCD-inspired quark models [2], the Hamiltonian generally includes a term of the form

$$H = \alpha_s c \sum_{i<j} \frac{1}{m_i m_j} \vec{s}_i \cdot \vec{s}_j \tag{7}$$

that is attractive in the spin singlet channel. Here $\vec{s}_i$ is the spin and m_i the (constituent) mass of the ith quark, and c is a constant. It follows that the strength of the interaction increases as quark masses decrease. For the purpose of quantifying the mass dependence of our wave functions, we define a ratio of RMS separations,

$$\mathcal{R}^{ud}_{us} = \sqrt{\frac{\langle|\vec{r}_u - \vec{r}_d|^2\rangle}{\langle|\vec{r}_u - \vec{r}_s|^2\rangle}}\,. \tag{8}$$

As noted earlier, fixed-gauge wave functions are generally broader in the Landau gauge than in the Coulomb gauge. For example, for the Λ state with $am_q = 0.03$ in the Landau gauge, we find $\sqrt{\langle|\vec{r}_u - \vec{r}_d|^2\rangle} = 5.63(6)$, as compared to 5.17(9) in the Coulomb gauge. Remarkably, however, ratios of separations appear to be rather independent of gauge.

In Fig. 7, we plot such ratios in both gauges for the two octet states and all available quark masses. By construction, the decuplet Σ^* is totally symmetric; the corresponding ratio is exactly one and would lie on the dotted line in the figure. We recall that in the Λ, the u, d are in the spin-0 configuration while in the Σ, the u, s and u, d are in superpositions of spin-0 and spin-1. Again, errors have been calculated with the bootstrap and leave little doubt that spatial correlations are enhanced in the scalar diquark channel. We also observe that the effect strengthens markedly at the lightest masses.

IV. DIQUARK MASSES

In the above sections, we have observed diquark effects via spatial correlations in baryon wave functions. An alternative approach for investigating diquarks on the lattice is to construct diquark-diquark correlators and fit their decay in Euclidean time in terms of an effective "diquark mass" [6]. This is not a gauge-invariant concept and such a parameter cannot be interpreted as the mass of a physical state, but it may nevertheless give some indication of the relative strength of binding. In [7], we presented results for diquark masses calculated in the Landau gauge from correlators of the form

$$G(t) = \sum_{\vec{r}} \langle \epsilon_{ijk} u_j(\vec{r},t) d_k(\vec{r},t) \epsilon_{ij'k'} \bar{u}_{j'}(\vec{0},0) \bar{d}_{k'}(\vec{0},0) \rangle\,, \tag{9}$$

where the indices label color, and implicit spin indices are assigned such that u,d are in either the spin-0 or spin-1 configuration. In Fig. 8, we reproduce a plot taken from [7], showing the dependence of diquark masses on quark mass. Also included is the "constituent quark mass," determined by performing a fit to the quark propagator in the Landau gauge. If one takes seriously this "constituent mass" interpretation, it appears that the scalar diquark may be bound in the limit of vanishing quark mass. Here we expand on these earlier results in two ways, by utilizing non-local sinks in the construction of the correlators and by reporting values for mass splittings, with errors taking into account correlations in the data.

In [7], diquark masses were extracted from point-to-point correlators. As discussed in Section II, we remain constrained to point sources, but we are free to use extended sinks, following the approach applied to mesons in [7]. A natural choice for this purpose is to use the diquark analogue of the baryon wave functions presented earlier, again calculated in the Landau gauge. In par-

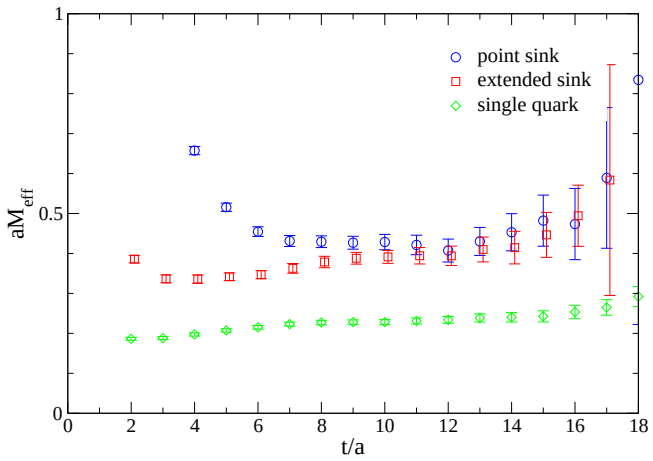

FIG. 9: (Color online) Effective mass of the scalar diquark as a function of time, calculated with both point and extended sinks. The effective quark mass is also shown.

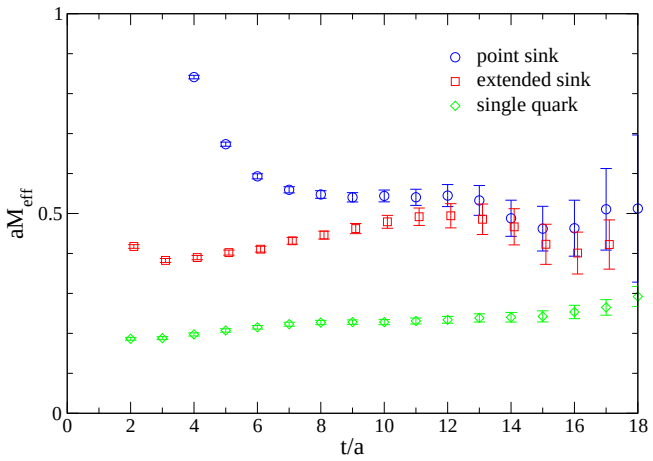

FIG. 10: (Color online) Effective mass of the vector diquark as a function of time, calculated with both point and extended sinks. The effective quark mass is also shown.

ticular, we generalize Eq. (9) to allow for a separation r between quarks at the sink,

$$G(r,t) = \sum_{\vec{r}_u,\vec{r}_d} \langle \epsilon_{ijk} u_j(\vec{r}_u,t) d_k(\vec{r}_d,t) \epsilon_{ij'k'} \bar{u}_{j'}(\vec{0},0) \times \bar{d}_{k'}(\vec{0},0)\rangle \delta(r - |\vec{r}_u - \vec{r}_d|)\,. \quad (10)$$

We take this function of r at $t = 10a$ to define the wave function, $\varphi(r) = G(r, 10a)$, calculating such a $\varphi(r)$ for each state and quark mass of interest. Finally, from these we construct an extended-sink correlator,

$$G_{\rm ext}(t) = \sum_r \varphi(r) G(r,t)\,, \quad (11)$$

whose fall-off yields the desired diquark mass.

In Fig. 9, we plot the effective mass of the scalar diquark as a function of time, given by $aM_{\rm eff} = -\ln[G(t)/G(t-a)]$, for both point-sink and extended-sink correlators. The bare quark mass is $am_q = 0.03$, our lightest value. The corresponding plot for the vector diquark is shown in Fig. 10. We find that both point and extended sink correlators display the same asymptotic effective mass, giving us confidence that the observed rate of exponential decay may be interpreted as the "mass" of the corresponding diquark in the Landau gauge. Results at heavier quark masses exhibit similar behavior. For the results that follow, we fit the extended-sink correlators in the region $11 \le t/a \le 14$ and calculate statistical errors by bootstrap.

We first consider the "binding" of the scalar diquark with respect to the combined mass of two "constituent quarks," indicated earlier in [7]. In Fig. 11, we plot the difference between the scalar diquark mass $M_{S=0}$ and twice the constituent quark mass M_Q. A naive linear extrapolation gives $a(M_{S=0} - 2M_Q) = -0.10(4)$ in the chiral limit.

A more robust feature than the binding of the scalar diquark is the large splitting between it and the vector

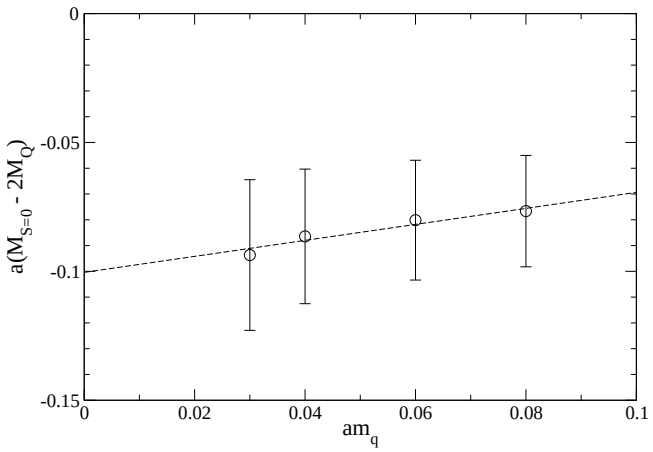

FIG. 11: Difference between the mass of the scalar diquark and twice the constituent quark mass, as a function of bare quark mass.

diquark. We plot our results for this mass difference in Fig. 12. A linear extrapolation to the chiral limit gives $a(M_{S=1} - M_{S=0}) = 0.077(35)$. Taking $a = 2.12$ GeV from the Sommer scale, we find $M_{S=1} - M_{S=0} = 162(75)$ MeV, where the error is statistical only. This splitting has also been calculated in [8, 9] in a gauge-invariant setup where the free color index of the diquark operator at source and sink is contracted with a Wilson line. Equivalently, this scheme corresponds to evaluating the diquark correlator in a temporal gauge, in which the temporal Wilson line reduces to the identity. Our different choice of gauge does not allow a direct comparison, but we note that the splitting is universally found to be positive and that it might be interesting to further investigate the gauge dependence of this quantity.

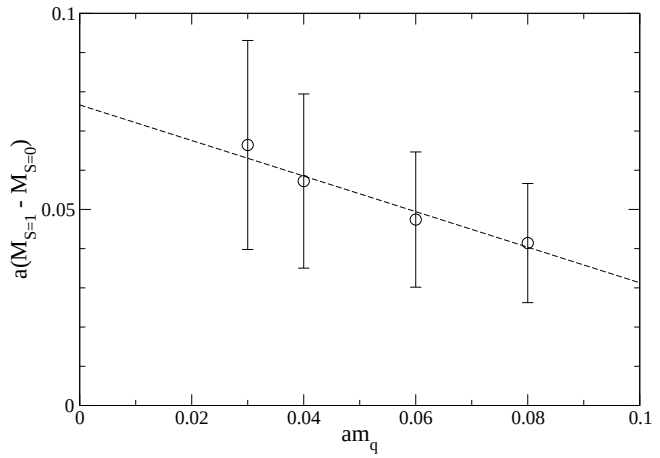

FIG. 12: Mass splitting between the scalar and vector diquark, as a function of bare quark mass.

V. CONCLUSIONS

In this work, we evaluated baryon wave functions in the Coulomb and Landau gauges and compared them on the basis of their diquark content. We found that spatial correlations were significantly enhanced between quarks in the scalar diquark configuration as compared to the vector diquark. Finally, we presented results for effective mass differences between diquark states calculated in the Landau gauge.

We acknowledge that our calculation suffers from limitations of the quenched approximation and the manifest gauge-dependence of our wave functions. It is encouraging, however, that enhanced correlations were equally pronounced in both gauges. It is also noteworthy that in all cases, diquark effects were found to become more pronounced as quark masses were decreased. This motivates further, preferably unquenched, calculations at lighter masses.

Acknowledgments

We thank Robert Jaffe and Frank Wilczek for stimulating discussions in the early stages of this investigation. This work is supported in part by US DOE grants DE-FG02-91ER40676 and DE-AC02-98CH10866, NSF grant No. DGE-0221680, EU RTN contracts No. HPRN-CT-2002-00311 (EURIDICE) and No. MRTN-CT-2006-035482 (FLAVIANET), and the CNRS GDR grant n° 2921 ("Physique subatomique et calculs sur réseau"). We thank Boston University and NCSA for use of their supercomputer facilities.

APPENDIX: TABLES OF QUARK SEPARATIONS

In Tables III and IV, we provide the root mean square separation between quarks in the various states, calculated as described in Sec. III B.

am_q	Λ		Σ		Σ^*
	$u-d$	$u-s$	$u-d$	$u-s$	$u-d$
0.03	5.63(6)	5.94(5)	6.03(5)	5.74(5)	6.05(5)
0.04	5.64(5)	5.93(4)	6.02(4)	5.74(4)	6.04(4)
0.06	5.63(4)	5.89(3)	5.98(3)	5.72(4)	6.01(3)
0.08	5.61(4)	5.85(3)	5.93(3)	5.69(3)	5.96(3)
0.10	5.58(3)	5.81(3)	5.88(3)	5.65(3)	5.92(3)
0.25	5.30(2)	5.45(2)	5.50(2)	5.35(2)	5.55(2)
0.50	4.76(2)	4.87(2)	4.91(2)	4.80(2)	4.97(2)
0.75	4.19(2)	4.30(2)	4.33(2)	4.23(2)	4.39(2)

TABLE III: RMS separation $\sqrt{\langle|\vec{r}_i-\vec{r}_j|^2\rangle}/a$, in lattice units, between quarks of flavor i and j as a function of bare quark mass, from baryon wave functions evaluated at $t = 10a$ in the Landau gauge.

am_q	Λ		Σ		Σ^*
	$u-d$	$u-s$	$u-d$	$u-s$	$u-d$
0.03	5.17(9)	5.46(8)	5.55(8)	5.27(8)	5.63(7)
0.04	5.19(7)	5.45(6)	5.53(6)	5.28(6)	5.61(6)
0.06	5.17(5)	5.41(5)	5.49(5)	5.25(5)	5.56(5)
0.08	5.14(5)	5.36(4)	5.43(4)	5.22(5)	5.50(4)
0.10	5.11(4)	5.31(4)	5.37(4)	5.17(4)	5.45(4)
0.25	4.78(3)	4.92(3)	4.97(3)	4.83(3)	5.04(4)
0.50	4.26(3)	4.36(3)	4.39(3)	4.29(3)	4.46(4)
0.75	3.75(3)	3.84(3)	3.87(3)	3.78(3)	3.94(3)

TABLE IV: RMS separation $\sqrt{\langle|\vec{r}_i-\vec{r}_j|^2\rangle}/a$, in lattice units, between quarks of flavor i and j as a function of bare quark mass, from baryon wave functions evaluated at $t = 10a$ in the Coulomb gauge.

[1] M. Anselmino, E. Predazzi, S. Ekelin, S. Fredriksson, and D. B. Lichtenberg, Rev. Mod. Phys. **65**, 1199 (1993).
[2] A. De Rujula, H. Georgi, and S. L. Glashow, Phys. Rev. **D12**, 147 (1975).
[3] R. L. Jaffe and F. Wilczek, Phys. Rev. Lett. **91**, 232003 (2003), hep-ph/0307341.
[4] M. Battaglieri, R. De Vita, and V. Kubarovsky (CLAS), AIP Conf. Proc. **806**, 48 (2006).
[5] R. L. Jaffe, Phys. Rept. **409**, 1 (2005), hep-ph/0409065.
[6] M. Hess, F. Karsch, E. Laermann, and I. Wetzorke, Phys. Rev. **D58**, 111502 (1998), hep-lat/9804023.
[7] R. Babich et al., JHEP **01**, 086 (2006), hep-lat/0509027.

[8] K. Orginos, PoS **LAT2005**, 054 (2006), hep-lat/0510082.
[9] C. Alexandrou, P. de Forcrand, and B. Lucini, Phys. Rev. Lett. **97**, 222002 (2006), hep-lat/0609004.
[10] Z. Liu and T. DeGrand (2006), hep-lat/0609038.
[11] B. Velikson and D. Weingarten, Nucl. Phys. **B249**, 433 (1985).
[12] S. A. Gottlieb (1985), presented at Conf. 'Advances in Lattice Gauge Theory', Tallahassee, FL, Apr 10-13, 1985.
[13] M. W. Hecht and T. A. DeGrand, Phys. Rev. **D46**, 2155 (1992).
[14] M. W. Hecht et al., Phys. Rev. **D47**, 285 (1993), hep-lat/9208005.
[15] K. Barad, M. Ogilvie, and C. Rebbi, Phys. Lett. **B143**, 222 (1984).
[16] K. Barad, M. Ogilvie, and C. Rebbi, Ann. Phys. **168**, 284 (1986).
[17] W. Wilcox, K.-F. Liu, B.-A. Li, and Y.-l. Zhu, Phys. Rev. **D34**, 3882 (1986).
[18] M. C. Chu, M. Lissia, and J. W. Negele, Nucl. Phys. **B360**, 31 (1991).
[19] M. C. Chu, J. M. Grandy, S. Huang, and J. W. Negele, Phys. Rev. **D49**, 6039 (1994), hep-lat/9312071.
[20] M. Burkardt, J. M. Grandy, and J. W. Negele, Ann. Phys. **238**, 441 (1995), hep-lat/9406009.
[21] C. Alexandrou, P. de Forcrand, and A. Tsapalis, Phys. Rev. **D66**, 094503 (2002), hep-lat/0206026.
[22] H. Neuberger, Phys. Rev. **D57**, 5417 (1998), hep-lat/9710089.
[23] H. Neuberger, Phys. Lett. **B417**, 141 (1998), hep-lat/9707022.
[24] R. Narayanan and H. Neuberger, Nucl. Phys. **B443**, 305 (1995), hep-th/9411108.
[25] R. Narayanan and H. Neuberger, Nucl. Phys. **B412**, 574 (1994), hep-lat/9307006.
[26] P. H. Ginsparg and K. G. Wilson, Phys. Rev. **D25**, 2649 (1982).
[27] M. Lüscher, Phys. Lett. **B428**, 342 (1998), hep-lat/9802011.
[28] R. Babich et al., Phys. Rev. **D74**, 073009 (2006), hep-lat/0605016.
[29] M. Guagnelli, R. Sommer, and H. Wittig (ALPHA), Nucl. Phys. **B535**, 389 (1998), hep-lat/9806005.
[30] S. Necco and R. Sommer, Nucl. Phys. **B622**, 328 (2002), hep-lat/0108008.
[31] R. Sommer, Nucl. Phys. **B411**, 839 (1994), hep-lat/9310022.
[32] P. Hernandez, K. Jansen, and M. Luscher, Nucl. Phys. **B552**, 363 (1999), hep-lat/9808010.